CHAPTER IV
RESULTS AND DISCUSSION

4.1 Electrospinning solution

Poly(vinyl alcohol) (PVA)/platinum nanoparticle nanocomposite nanofibers were successfully prepared via the electrospinning technique. A platinum precursor, chloroplatinic acid hexahydrate ($H_2PtCl_6.6H_2O$), was reduced to Pt metal particles directly in 8% PVA viscous solution by citrate ions (Lin *et al.*, 2005) under 95-100 °C and vigorous stirring as follows:

$$PtCl_6^{2-} + Cit^- + H_2O \rightarrow Pt^0 + CO_2 + H^+ + Cl^- \quad (4.1)$$

A clear yellow solution of CPAH ($PtCl_6^{2-}$) became dark brown which referred to the presence of Pt metal after the reduction process has been carried out. However, PVA fine powder was added twice. Firstly, small amount of PVA added served as a stabilizer to prevent an aggregation of Pt nucleuses generated during chemical reduction. Later, more PVA was added in order to form as-spun fibers. In addition, if large amount of PVA was added at once, long PVA chains (molecular weight = 72,000) would restrict chemical reaction between chloroplatinic acid hexahydrate and citrate ions giving small content of Pt nanoparticles generated (Bai *et al.*, 2007).

PVA has high viscosity due to strong intermolecular hydrogen bonding between PVA chains and between PVA chains and water molecules. Strong intramolecular hydrogen bonding between hydroxyl groups on the same PVA chains also affects the solution viscosity. Other than hydrogen bonding, PVA applied in the experiment had high molecular weight (72,000) which could cause high degree of entanglement. As Pt metal occurred in the system, solution concentration was increased. Moreover, the attraction force between Pt and lone pair electron on hydroxyl groups took place promoting the viscosity of the solution. Hence, when Pt content was increased, viscosity of the solution was increased as shown in table 4.1.

Table 4.1 Solution viscosity of solutions with different Pt loadings.

Pt loading (wt.%)	0	1	3	5
Average Viscosity (cP)	192.7 ± 1.53	219.0 ± 5.29	260.0 ± 5.13	333.0 ± 3.00

The UV-Vis spectra in figure 4.1 shows the UV absorption of different solutions including pure precursor, 1%, 3% and 5% Pt loadings before reduction reaction took place. An absorption band at 260 nm corresponds to Pt^{4+} contained in each solution (Lin *et al.*, 2006). In pure precursor solution, high concentration of Pt^{4+} showed higher absorption of the band at 260 nm compared to lower concentrated solutions, 5%, 3% and 1%, respectively.

Figure 4.2 demonstrates the UV absorption property of prepared solution with 1% Pt loading at different reduction times. At 0 minute or before reaction started, the absorption band at 260 nm was observed due to the presence of Pt^{4+} in the solution as mentioned above. On the other hand, when reduction reaction with citrate salts had taken place after 30 minutes, the bands at 260 nm disappeared which suggested that $H_2PtCl_6.6H_2O$ was completely reduced to metal form, suspended and stabilized in the aqueous solution as dark brown solution was obtained. Longer reduction time gave higher absorption band due to larger amount of Pt particles produced in the system scattered the UV radiation provided. In addition, the absorption bands tended to increase towards the shorter wavelengths in UV range due to the surface Plasmon of platinum nanoparticles (Chen *et al.*, 2007).

Figure 4.3 and 4.4 illustrates the UV absorption property of prepared solution with 3% and 5% Pt loadings at different reduction times. The results were similar to those observed in 1% Pt loading. Moreover, in figure 4.5-4.8, more platinum precursor loaded gave higher UV absorption bands at different reaction times according to more Pt nanoparticles generated in the systems.

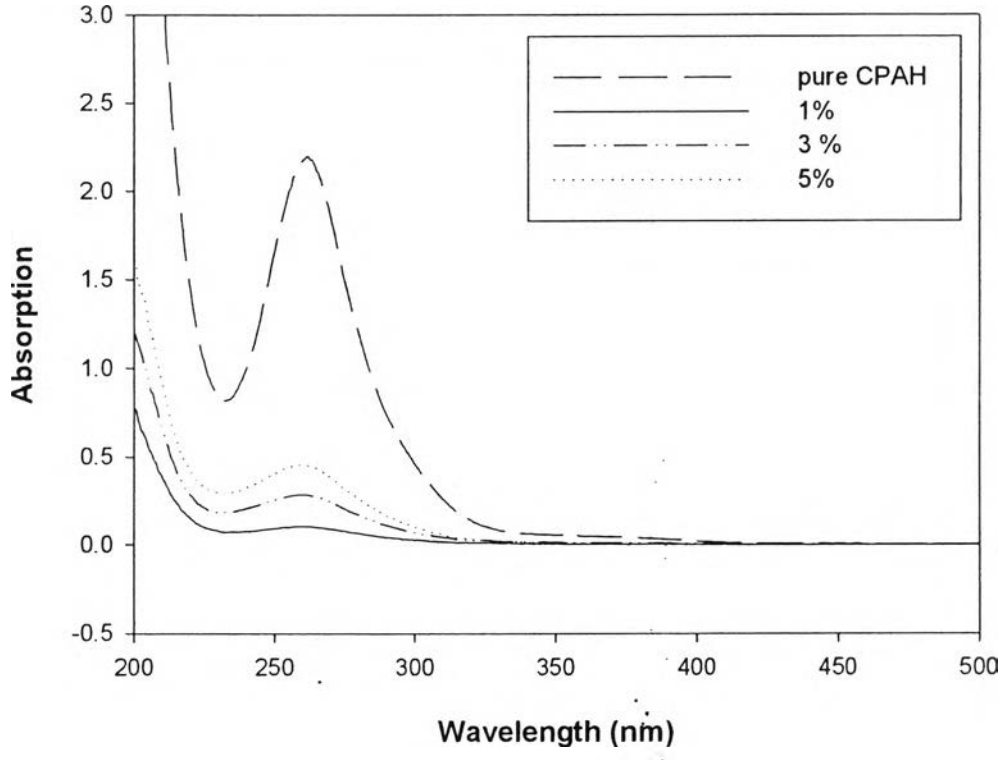

Figure 4.1 UV-Visible absorption spectra of aqueous solution of pure precursor, 1 %, 3% and 5% Pt loading before chemical reduction.

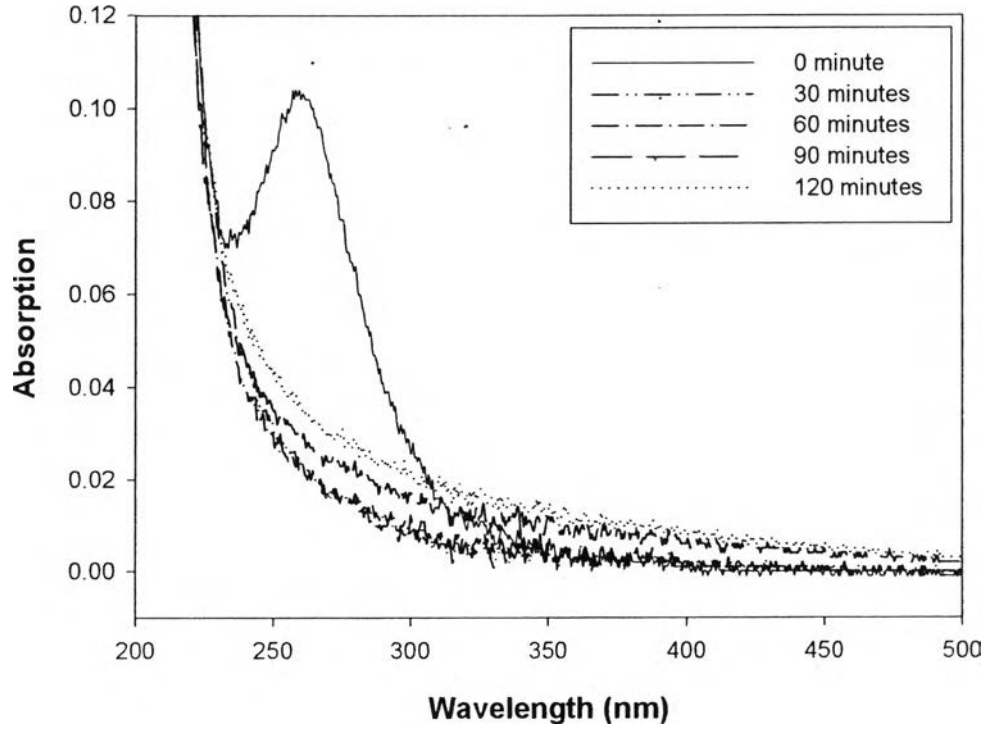

Figure 4.2 UV-Visible absorption spectra of aqueous solutions of 1 %wt Pt loading at different reaction times.

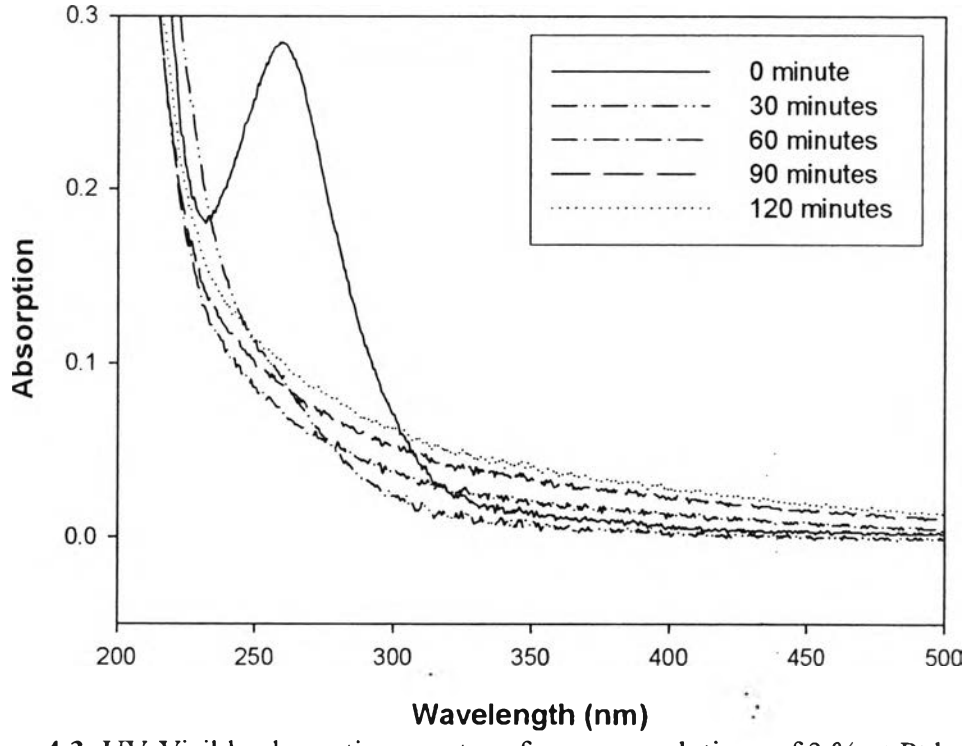

Figure 4.3 UV-Visible absorption spectra of aqueous solutions of 3 %wt Pt loading at different reaction times.

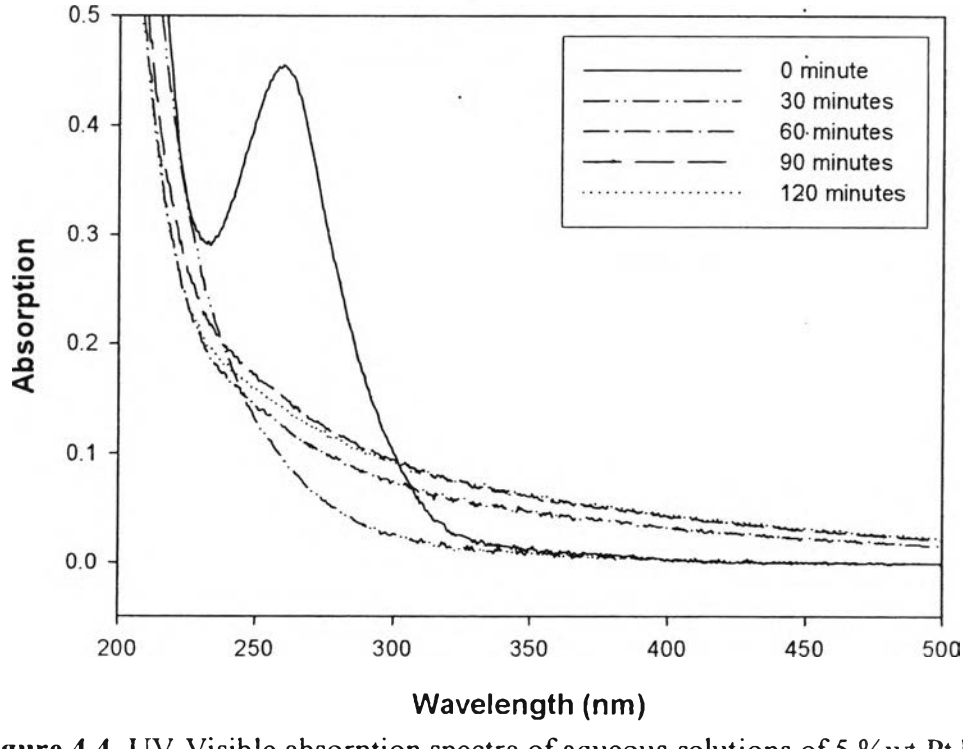

Figure 4.4 UV-Visible absorption spectra of aqueous solutions of 5 %wt Pt loading at different reaction times.

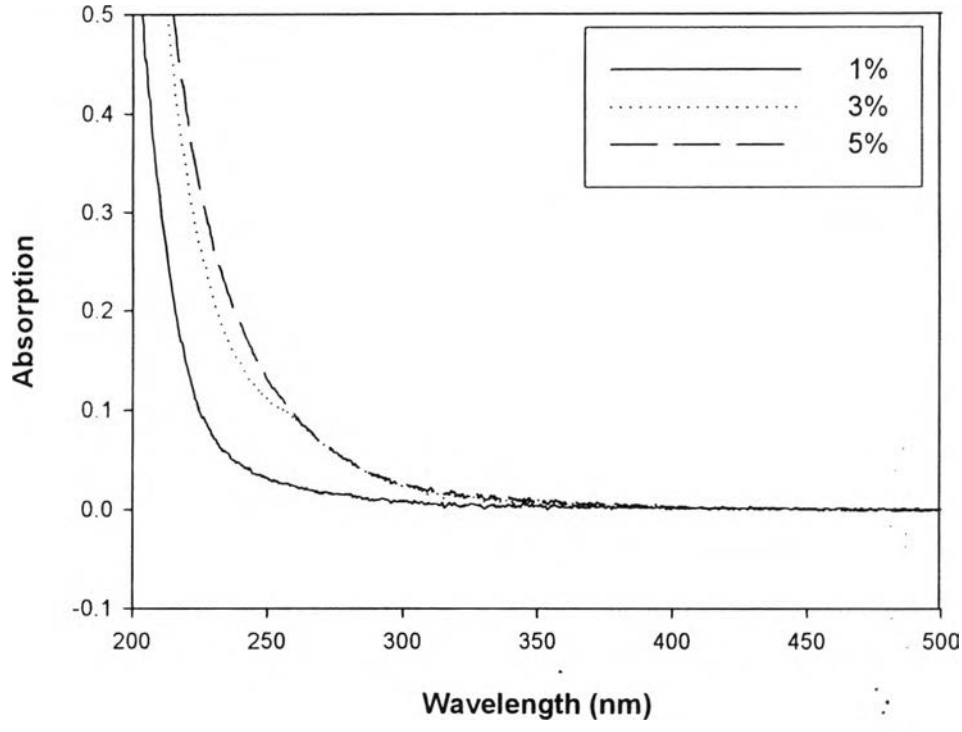

Figure 4.5 UV-Visible absorption of viscous solution with different % Pt loading after 30 minutes reduction process.

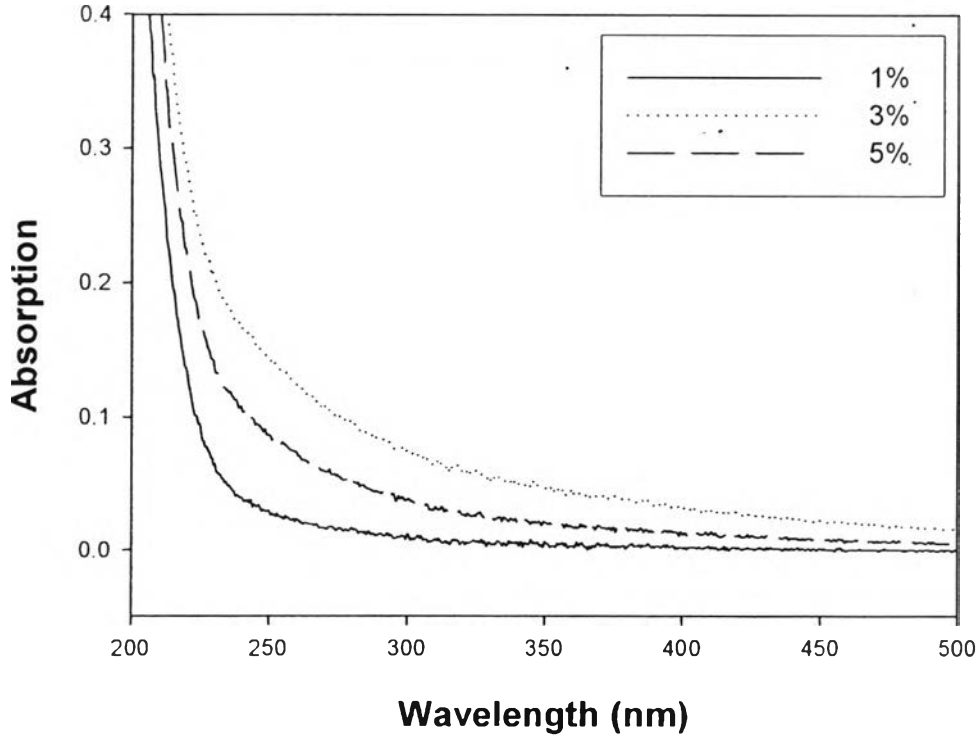

Figure 4.6 UV-Visible absorption of viscous solution with different % Pt loading after 60 minutes reduction process.

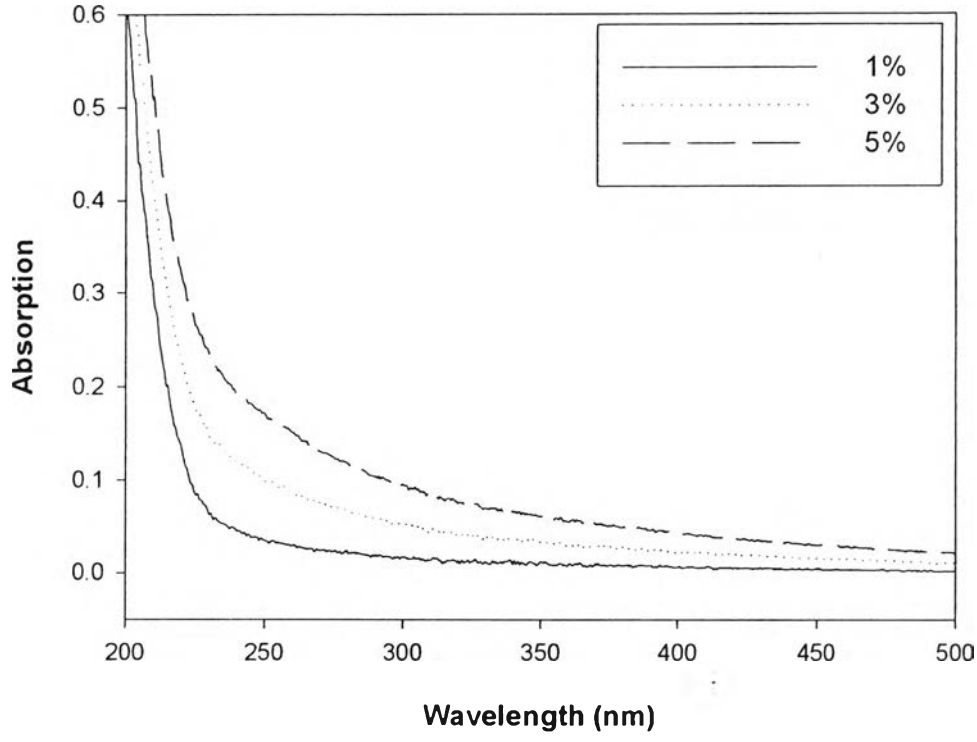

Figure 4.7 UV-Visible absorption of viscous solution with different % Pt loading after 90 minutes reduction process.

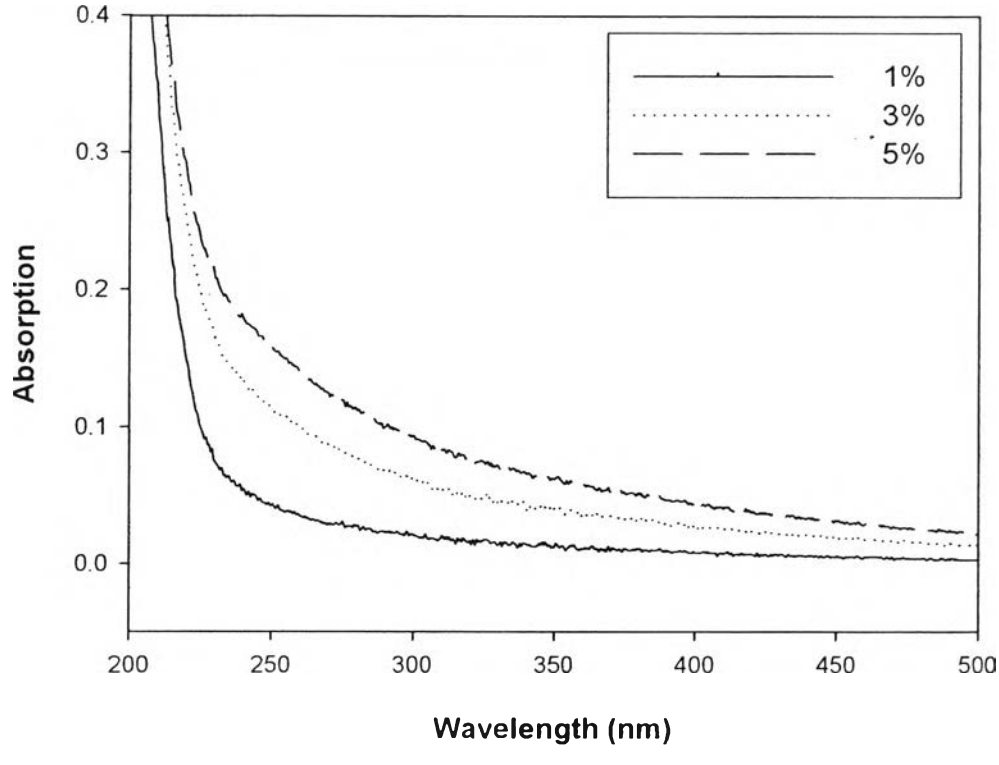

Figure 4.8 UV-Visible absorption of viscous solution with different % Pt loading after 120 minutes reduction process.

After the electrospinning solution was prepared, the solution was subjected to an electrospinning set up. The solution was exposed to high voltage of 17 kV at a nozzle where solution jet was ejected out. The collector was 15 cm away from the nozzle. Sodium dodecyl sulfate (SDS), a surfactant, promotes electrospinning process by lowering the surface tension of the Pt/PVA solution which had high surface tension according to strong hydrogen bonding and high viscosity. Without SDS, non-continuous jet would be obtained and since PVA is sensitive to moisture, solution would easily solidify and block the solution flow at the nozzle. In addition, voltage used of 17 kV was low, compared to the voltage applied in other studies (Tao and Shivkumar, 2007 and Koski *et al.*, 2004). This was due to higher conductivity of the electrospinning solution with the presence of Pt metal.

4.2 Morphology

The average diameters of the nanocomposite nanofibers observed from SEM images in figure 4.9 were between 170 and 274 nm calculated by SemAfore. For Pt loading of 1 wt%, an average diameter observed was 274.1 nm. Likewise, Pt loading of 3 wt%, and 5 wt% gave as-spun average diameters of 187.2 and 169.3 nm, respectively. The average diameters were decreased when amount of Pt loading was increased. The results corresponded to an increasing of charge density when more Pt precursor was added because Pt in metal form has high conductivity. Higher conductivity caused higher elongation of the ejected jet of the electrospinning solutions in an electrical field towards the metal collector and led to smaller fiber formation (Bai *et al.*, 2007). The histograms plotted in figure 4.10 indicate that Pt nanoparticle impregnated PVA nanofibers with 5% Pt loading exhibited narrowest size distribution of PVA nanofiber diameter. On the other hand, PVA with 5% Pt loading gave more non-uniform and rougher surface as-spun fibers compared to as-spun fibers from other conditions. This could possibly be affected by very high conductivity of electrospinning solution, thus ejected jet traveled to the collector too fast and solvent had insufficient time to evaporate out off the fibers. As-spun pure PVA showed small diameter of 90.7 nm. Some breakage and beads can also be observed. Therefore, some Pt nanoparticles can ease the electrospinning of PVA.

Table 4.2 Average diameters of as-spun fibers from different % Pt loadings.

% Pt loading	0	1	3	5
Average Diameter (micron)	0.0907 ± 0.027	0.2741 ± 0.073	0.1872 ± 0.041	0.1693 ± 0.034

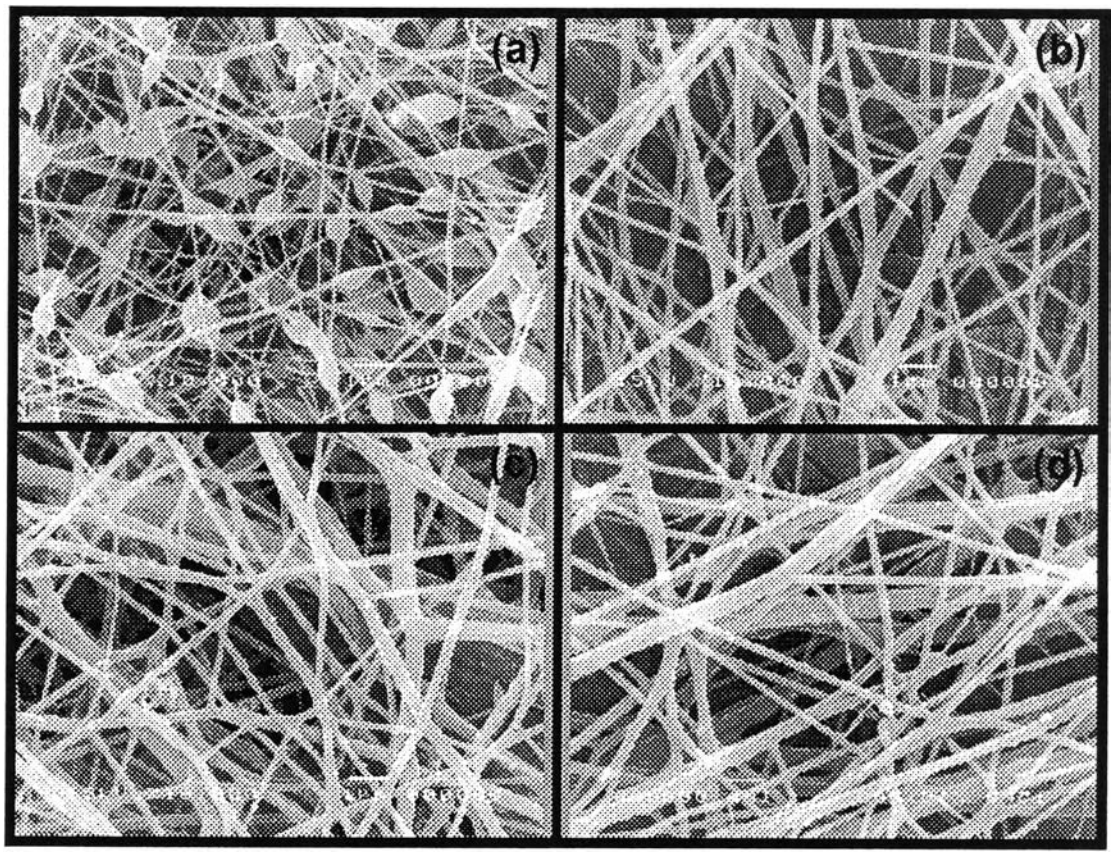

Figure 4.9 SEM images of composite fibers with different %Pt loadings (a) pure PVA, (b) 1%, (c) 3%, and (d) 5%.

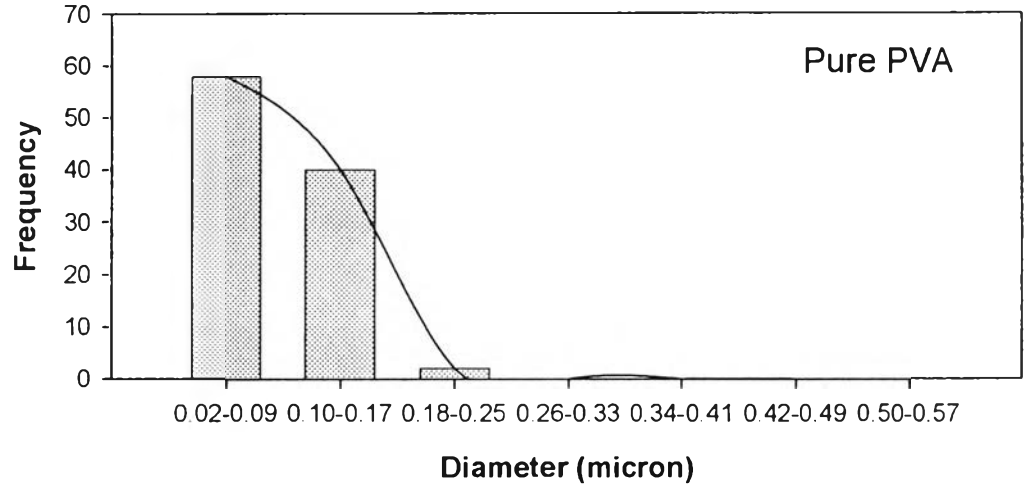
Pure PVA
Frequency
70
60
50
40
30
20
10
0
0.02-0.09
0.10-0.17
0.18-0.25
0.26-0.33
0.34-0.41
0.42-0.49
0.50-0.57
Diameter (micron)

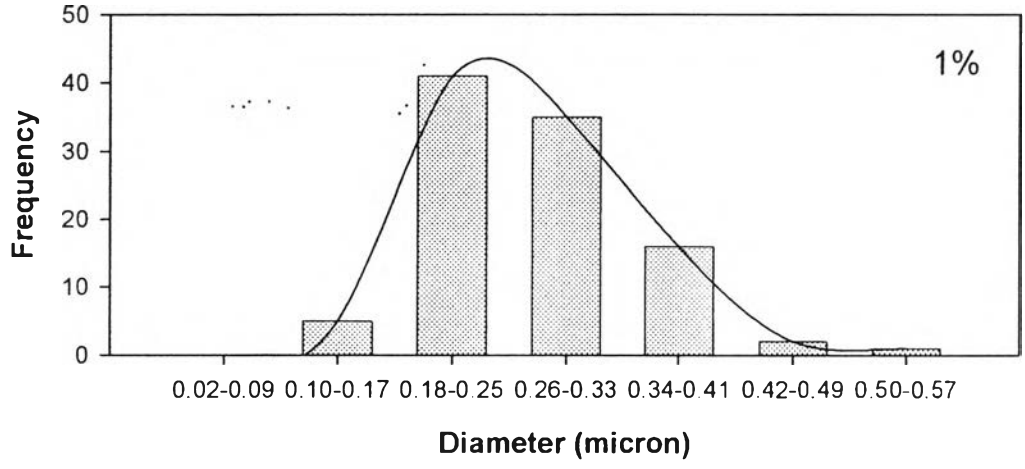
1%
Frequency
50
40
30
20
10
0
0.02-0.09
0.10-0.17
0.18-0.25
0.26-0.33
0.34-0.41
0.42-0.49
0.50-0.57
Diameter (micron)

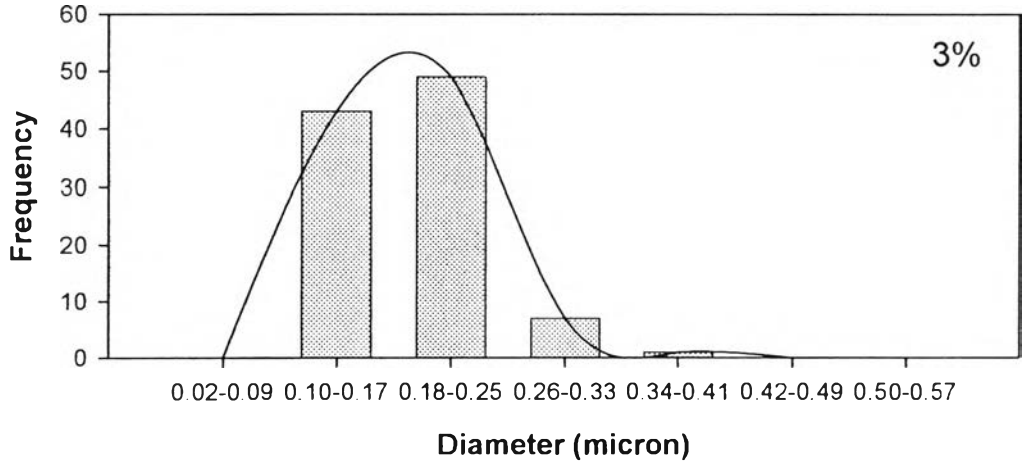
3%
Frequency
60
50
40
30
20
10
0
0.02-0.09
0.10-0.17
0.18-0.25
0.26-0.33
0.34-0.41
0.42-0.49
0.50-0.57
Diameter (micron)

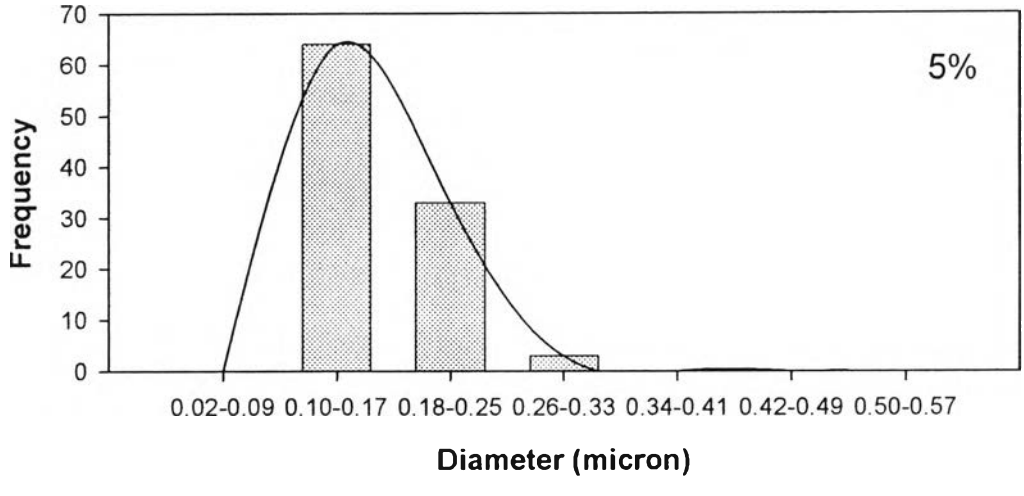

Figure 4.10 Histograms showing size distribution of fiber diameters of Pure PVA, 1%, 3% and 5% Pt loadings.

TEM images in figure 4.11 demonstrated that the increasing in chloroplatinic acid hexahydrate content, more Pt particles were produced in the fibers. From the excess of reducing agent, tri-sodium citrate, more precursor added can also be reduced completely giving larger amount of the particles generated in the fibers. It was also observed that the surface of the fibers obtained were smooth. An average diameter of the Pt particles obtained was in range of 1-6 nm. The pure PVA fiber in figure 4.11(a) had bright color compared to the other fibers containing Pt nanoparticles which exhibited darker fibers. TEM images from PVA with 1%, 3% and 5% Pt contents showed some darker zones which were believed to be groups of individual Pt nanoparticles.

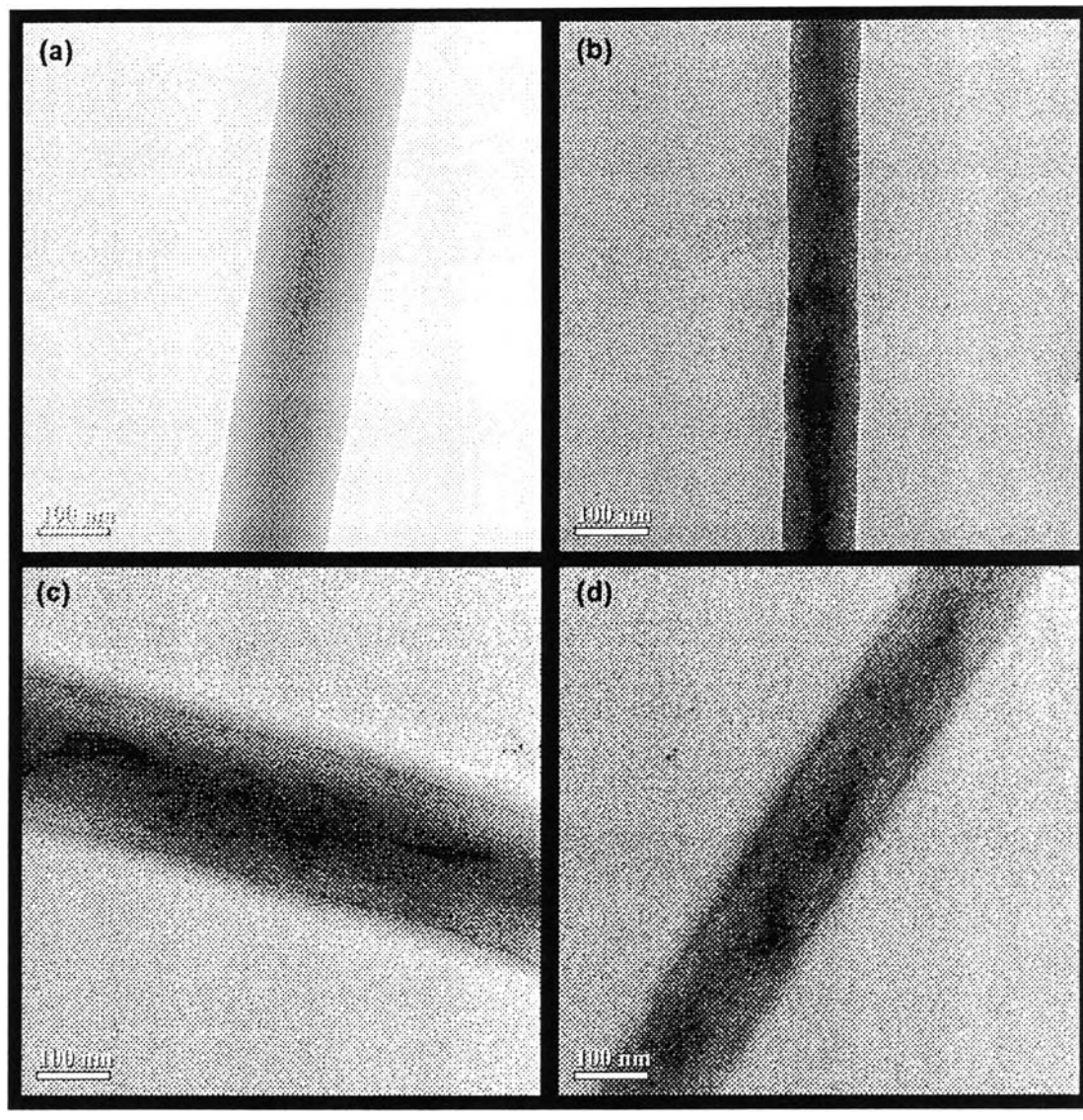

Figure 4.11 TEM images of Pt incorporated nanofibers from pure PVA and PVA templates with different %wt Pt loadings; (a) pure PVA, (b) 1%, (c) 3%, and (d) 5%.

4.3 Characterization of Pt nanoparticles

Table 4.3 Pt content in each fiber mat obtained from XRF-EDX spectrum.

% Pt loading	sample number	Pt content in a fiber mat (ppm)	Average	SD
Pure	1	0.04	0.468	0.866
	2	0		
	3	0		
	4	2		
	5	0.3		
1%	1	491	462.4	117.076
	2	291		
	3	401		
	4	567		
	5	562		
3%	1	1214	1158.8	290.843
	2	1499		
	3	1242		
	4	1141		
	5	698		
5%	1	1317	1421.4	210.424
	2	1468		
	3	1220		
	4	1763		
	5	1339		

From XRF-EDX results in table 4.3, it was found that 1%, 3% and 5% Pt loadings gave Pt nanoparticles content of 462.4, 1158.8, and 1421.4 ppm respectively. The increasing in precursor content caused larger Pt nanoparticles composition on the PVA fiber mats.

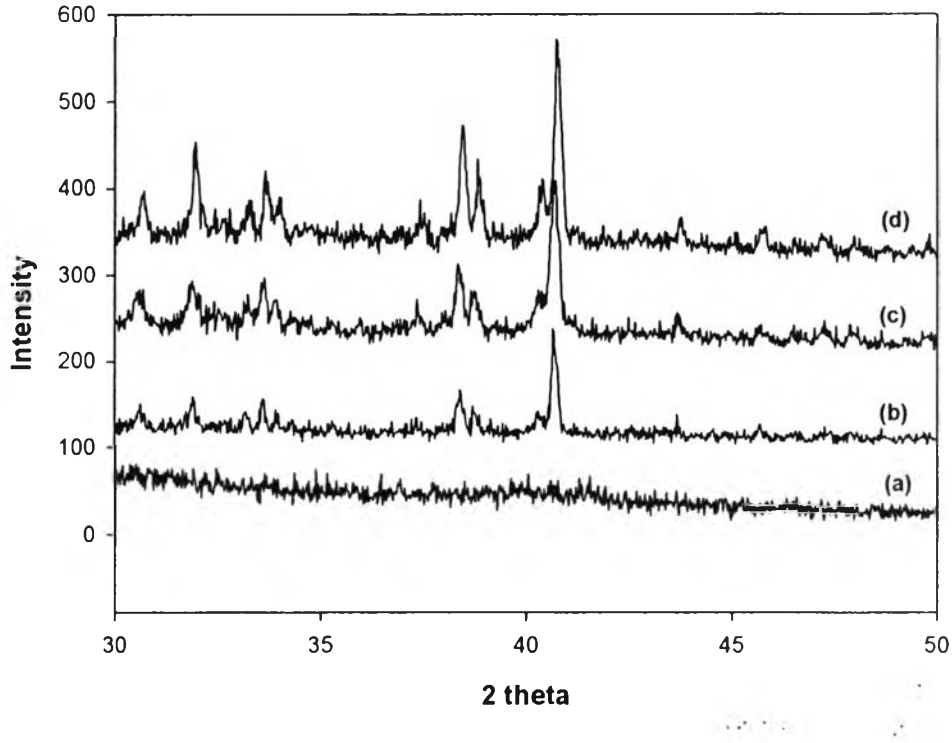

Figure 4.12. XRD of Pt/PVA nanocomposite nanofibers at different Pt loadings: (a) pure PVA, (b) 1%, (c) 3%, and (d) 5%.

Another way to confirm the occurrence of Pt element in the PVA fiber mats is XRD. The XRD results, figure 4.12, the diffraction around $2\theta \sim 40°$ could be indexed to (1 1 1) reflection of face-centered-cubic phase of platinum bulk (Jiang *et al.*, 2006). As the Pt content increased, the intensity of the peak gradually increased. Usually Pt shows reflections of (1 1 1), (2 0 0), (2 2 0), (3 1 1) and (2 2 2), but in this experiment, (1 1 1) plane was significant. It can be attributed to very small Pt nanoparticles obtained.

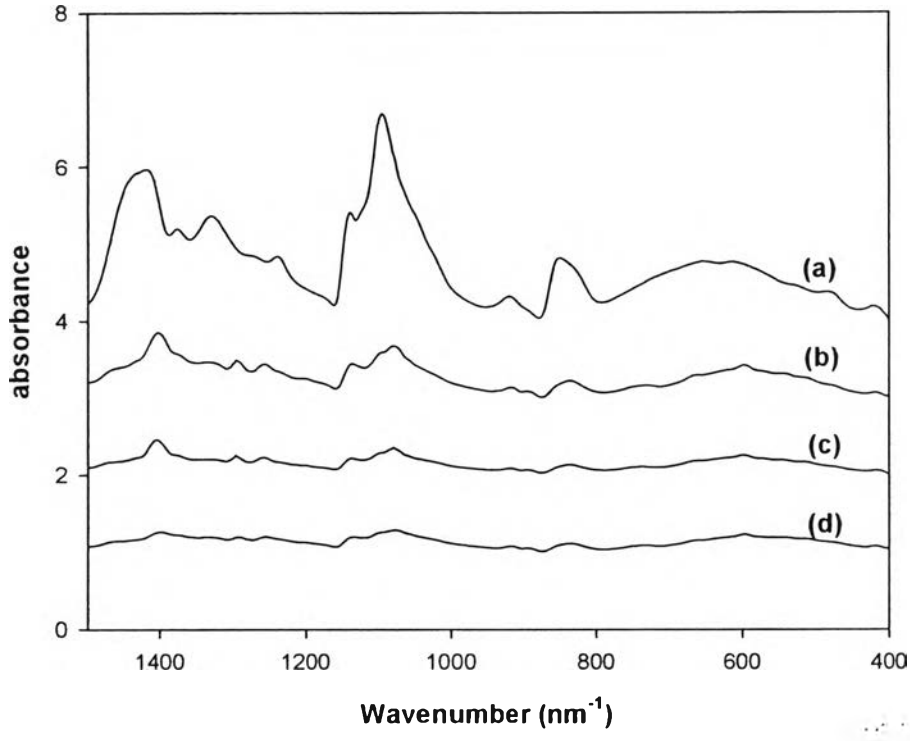

Figure 4.13 FTIR spectra of pure PVA mat and PVA nanofibers with different Pt loadings: (a) pure PVA, (b) 1%, (c) 3%, and (d) 5%.

Other than an observation of the small black particles attached to the fibers in TEM images, the existence of Pt nanoparticles was also confirmed by EDX and XRD techniques.

According to the FTIR spectra in figure 4.13, the band at 618 cm^{-1}, out-of-plane vibration of O-H groups and the band at 849 cm-1 which referred to C-H bonds that vibrates out-of-plane, those bands gradually decreased as the more Pt was loaded. Also, absorption bands at 1331 cm^{-1} and 1418 cm^{-1} which respectively belonged to the coupling of O-H in plane vibration and C-H wagging vibrations were slightly weakened. Moreover, from figure 4.8,indicated that the intensity of alkane bands, the bands at 2939 cm^{-1} and 2911cm^{-1}, and hydroxyl bands, the band at 3322 cm^{-1}were decreased while Pt content in PVA nanofiber mat were increased. This suggested that some bonds between PVA templates and Pt nanoparticles replaced hydroxyls groups on PVA chains.

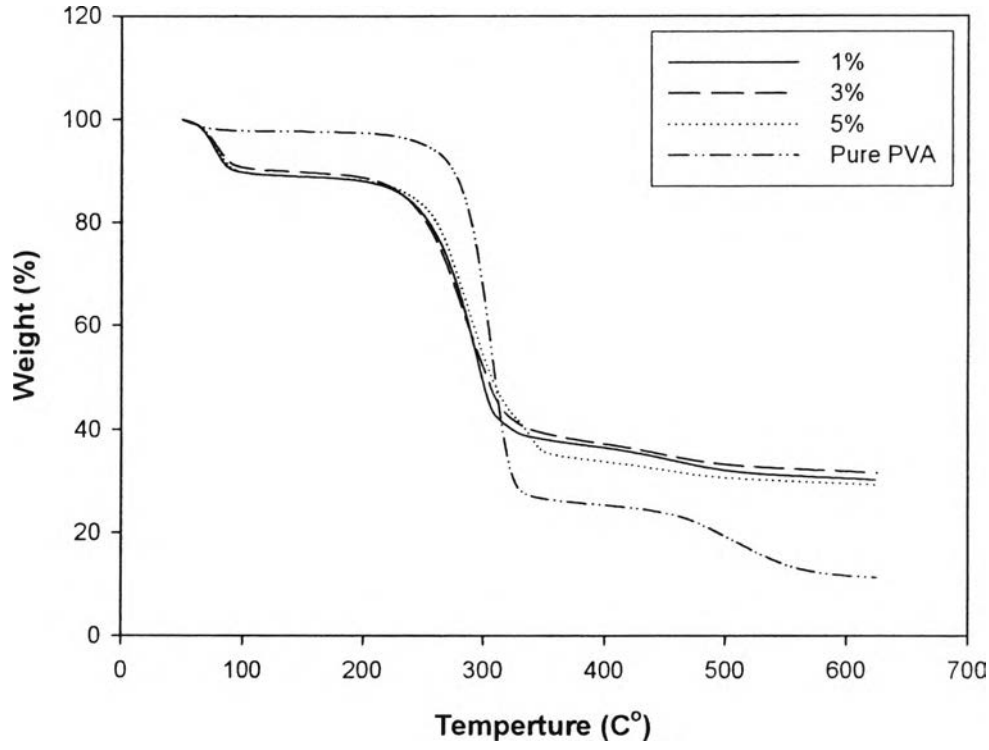

Figure 4.14 TGA thermograms of PVA pure and PVA with different Pt contents.

Thermogravimetric analysis was applied to investigate thermal property of the nanocomposites nanofibers, degradation behavior, under heating rate of 10 °C min^{-1}. Temperature was swept from 50-600 °C under N_2 atmosphere. From 50-100 °C, the thermograms (figure 4.14) showed the loss of water which water content was high in PVA containing Pt nanoparticles, whereas a small amount of water elimination in pure PVA was observed. The loss was due to some moisture contained on the fiber mats as PVA is a water-soluble polymer. Pure PVA exhibited 2-step degradation (Peng and Kong, 2007) while the nanocomposite nanofibers showed 1-step degradation. The first step degradation in pure PVA (250-350 °C) involves chain stripping elimination of H_2O and the chain-scission reactions which occur in parallel. The products of the first step are polyenes from the chain-stripping elimination reaction of H2O, also *cis* and *trans* allylic-methyls that may form from random chain scission that takes place with an elimination. The second step (450-550 °C), cyclization (Diels-Alder intramolecular and intermolecular cyclization followed by dehydrogenation with aromatization) and radical reaction pathways, which occur in

parallel, are responsible for the conversion of unsaturated carbons into substituted aromatic or aliphatic carbons (Krklješ *et al.*, 2007).

Two general mechanisms are probably responsible for the modes of action of Pt nanoparticles on the thermal degradation of PVA. One is described as a chemical constraint for the H_2O elimination in the first degradation step due to the interaction of Pt nanoparticles with OH groups, which may increase energy barrier of the chain-stripping elimination reaction of H_2O and induce a shift of the thermal degradation of partial decomposition products toward chain scission and formation of methyl terminated polyenes. In addition, the interaction of OH groups with Pt nanoparticles is confirmed by FTIR spectra which were discussed earlier. Pt nanoparticles may act as radical scavenger suppressing radical transfer to the adjacent chains via intermolecular and intramolecular chain reactions. The second mechanism is a physical constraint (reduced molecular mobility) for the reactions of inter and intra cyclization of polyenes in the second degradation step that seem to occur preferably at a lower heating rate compared with radical reaction pathways.

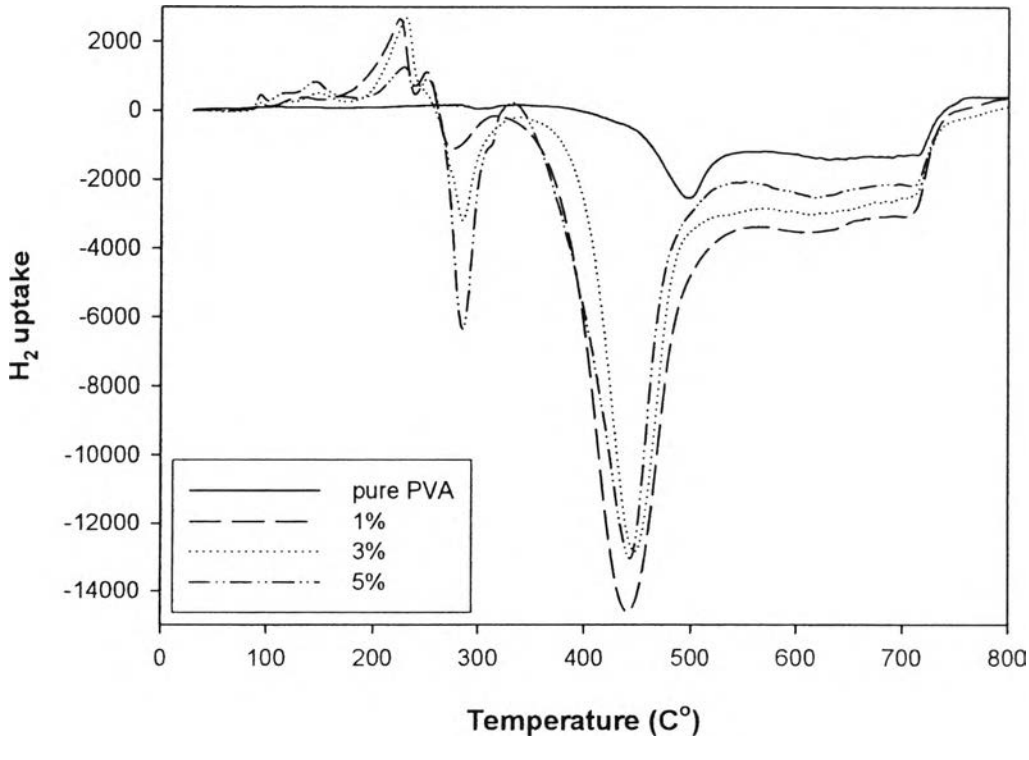

Figure 4.15 TPR of Pt/PVA nanocomposite nanofibers with different Pt loadings.

Figure 4.15, a pure PVA and nanocomposites nanofiber flakes were heated under hydrogen atmosphere from 30-700 °C. The pure PVA gave a flat line before 350 °C was reached. No hydrogen was absorbed; instead, pure PVA gave out some hydrogen gas after 350 °C according to the degradation of PVA at elevated temperature. The spectra of nanocomposite nanofibers with 1%, 3% and 5% Pt loadings showed hydrogen absorption peaks about 100 °C and 200 °C, also hydrogen desorption peaks were observed at about 300 °C and 445 °C. A small reduction peak at about 100 °C followed by a broader main peak centered at 200 °C were observed for Pt/PVA due to the reduction of platinum oxide generated from being oxidized by oxygen in the atmosphere during electrospinning process. From Pieck et al. (2001), the TPR spectra of PtO_x usually exhibit two reduction peaks at about 100 °C and 200 °C. However, the peak positions detected slightly shifted according to the interaction between Pt particles and support molecules. Therefore, some Pt ions were completely reduced from Pt^{4+} to either metal form or oxide form, . Pt in oxide form was reduced again by hydrogen gas supplied and transferred to metal form eventually. The desorption peaks, at 300 °C and 445 °C, were also corresponding to the degradation of the PVA templates supporting Pt nanoparticles.